International Journal of Chemical, Materials and Biomolecular Sciences
ISSN: 2415-6620
Vol:10, No:6, 2016

Numerical Study of Developing Laminar Forced Convection Flow of Water/CuO Nanofluid in a Circular Tube with a 180 Degrees Curve

Hamed K. Arzani, Hamid K. Arzani, S.N. Kazi, A. Badarudin

***Abstract*—**Numerical investigation into convective heat transfer of CuO-Water based nanofluid in a pipe with return bend under laminar flow conditions has been done. The impacts of Reynolds number and the volume concentration of nanoparticles on the flow and the convective heat transfer behaviour are investigated. The results indicate that the increase in Reynolds number leads to the enhancement of average Nusselt number, and the increase in specific heat in the presence of the nanofluid results in improvement in heat transfer. Also, the presence of the secondary flow in the curve plays a key role in increasing the average Nusselt number and it appears higher than the inlet and outlet tubes. However, the pressure drop curve increases significantly in the tubes with the increase in nanoparticles concentration.

***Keywords*—**Laminar forced convection, nanofluid, curve, return bend, CFD.

I. Introduction

RECENTLY, almost all the advances and developments in industrial technology are focusing on reducing system processes that lead to higher power concentrations for a wide range of applications. Consequently, the need for an increase in cooling capacities has been vital for these compact thermal systems. The conventional methods, for example the use of extension surfaces like fins or utilizing micro channels with high heat transfer surface, are designed to obtain the desired high cooling efficiency. On the other hand, the cooling fluid characteristics have been taken into consideration.

Nanofluid is defined as a new kind of fluid with metallic nanoparticles suspended in liquid molecules. Heat transfer in nanofluid can be functions of dimension, properties, solid volume concentration of nanoparticles etc. According to experimental investigations [1]-[5], nanofluids have shown a significant potential for augmentation of energy transfer and also have higher thermal conductivities in comparison to the base fluids.

The term nanofluid was used by Choi in 1995 [6]. After that, many studies focused on the nanofluids flow its thermophysical properties [2]-[5], [7]. Most of the researchers focused on the modelling of the effective thermal conductivity of nanofluids [8]-[12]. Subsequent research stated that nanofluids also have other appropriate behaviours and properties such as higher forced convection heat transfer [13]-[17], increased spreading and wetting [18],[19], and improved critical heat fluxes in boiling situation [20]. However, there are disagreements in the literature in terms of the extent of thermal conduction improvement in static conditions, the mechanisms of heat transfer improvement in various conditions, the effect of the presence of nanoparticles on nucleate boiling heat transfer and natural convection [21]-[25].

The objective of the current investigation is to analyse the thermal and hydrodynamic characteristics of the CuO-Water based nanofluid in a pipe with a return bend. The FVM (finite volume method) has been employed to solve the governing equations for the fluid and thermal flows. Fluid properties are considered to be temperature dependent. To predict the heat transfer behaviours of the nanofluid, the Nusselt numbers will be considered with the Reynolds numbers of 10, 250, 500, 750, and 1000 and the nanoparticle volume fractions of 0, 2, 4, 6, and 8%. The temperature and velocity distributions will be achieved to figure out the role of the curve, and the pressure drop will be measured to understand the influence of the nanofluid viscosity.

II. Methodology

A. Geometry Structure and Boundary Conditions

Two cylindrical tubes in horizontal position with diameters of 10 mm and the lengths (l) of 100 mm, and a 180 degree curve with the radius of 15 mm are considered in the present study. The two-dimensional (2D) geometry has been applied. Fig. 1 shows the geometrical configuration taken under study. The detail of setup and numerical parameters are illustrated in Fig. 2.

B. Mesh and Mesh Dependency Test

The meshing tool available in ANSYS was used to construct the computational mesh. A structured mesh based on a rectangular grid was used throughout the domain. Several grid distributions had been tested and the results were compared to ensure that the calculated results were grid independent. Fig. 3 draws the comparison of Nusselt numbers versus the Reynolds numbers based on water for three different grid distributions. It is shown that all these results are independent of the number of grid points. To reduce

Hamed K. Arzani is with department of Mechanical Engineering, University of Malaya, Kuala Lumpur, Malaysia (phone: +601762702920; e-mail: hamedarzani@um.edu.my).

Hamid K. Arzani is with aerospace department, Malek-Ashtar University of Technology, Isfahan, Iran (e-mail: hkh_arzani@yahoo.com).

S.N. Kazi is with department of Mechanical Engineering, University of Malaya, Kuala Lumpur, Malaysia (phone: + 603-7967 4582; e-mail: salimnewaz@um.edu.my).

A. Badarudin is with department of Mechanical Engineering, University of Malaya, Kuala Lumpur, Malaysia (e-mail: ab01@um.edu.my).

computational time and effort, the total grid points and the elements employed in the whole tube are 25551 and 25000, respectively. A non-uniform grid was used in the meshing step, close to the wall grids are smaller to get better results.

Fig. 1 Geometrical configuration of the present study

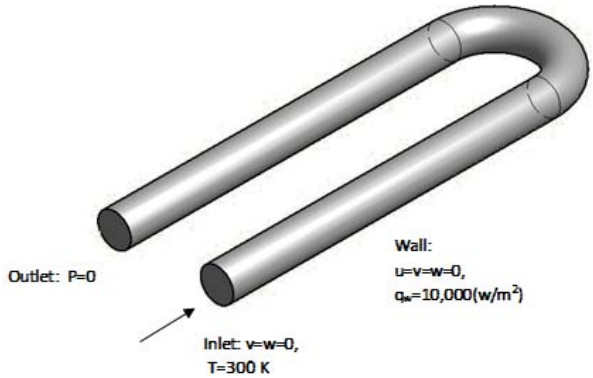

Fig. 2 Boundary conditions for the tubes with 180 degree curve

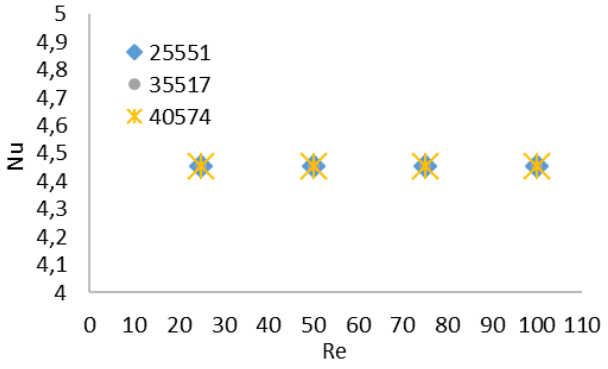

Fig. 3 Comparison of Nusselt numbers versus Reynolds numbers for water at three different grid distributions

C. Governing Equations

A general approach is the single phase model, which is considered for the current study. The nanoparticles in the base fluid may be easily fluidized and consequently the effective mixture behaves like a single phase fluid [26]. It is also assumed that the fluid phase and the nanoparticles are in thermal equilibrium with zero relative velocity. This may be realistic as nanoparticles are much smaller than micro particles and the relative velocity decreases with the decrease in particle size. The resultant mixture may be considered as a conventional single phase fluid [11]. Considering the laminar forced convection of a steady flow incompressible and Newtonian fluid, the governing equations for the single phase model can be written as follows [27],

Continuity equation:

$$\nabla.(\rho_{eff} V) = 0 \tag{1}$$

Momentum equations:

$$\nabla.(\rho_{eff} VV) = -\nabla P + \mu_{eff} \nabla^2 V \tag{2}$$

Conservation of energy:

$$\nabla.(\rho_{eff} C_{p,eff} VT) = \nabla.((k_{eff})\nabla T) \tag{3}$$

TABLE I
WATER AND CUO PHYSICAL PROPERTIES

	Density (Kg/m^3)	Viscosity (Ns/m^2)	Specific heat ($J/Kg^{\circ}K$)	Conductivity ($W/m^{\circ}K$)	Shape factor (n)
CUO	6500	-	535.6	20	3

Table I shows the physical properties of CuO nanoparticle. The thermal conductivity of CuO is larger than base fluid (water) and it is reasonable for the increasing heat transfer characteristics of CuO-water based nanofluid. The following equations for water properties are used:

- Density [28]

$$\rho_f = 2446 - 20.674T + 0.11576T^2 - 3.12895\times10^{-4}T^3 + 4.0505\times10^{-7}T^4 - 2.0546\times10^{-10}T^5 \tag{4}$$

- Viscosity [3]

$$\mu_f = A10^{(\frac{B}{T-C})} \tag{5}$$

where $A = 2.414\times10^{-5}$, $B = 247.8$ and C=140.

- Specific heat [28]

$$(C_p)_f = \exp\left(\frac{8.29041 - 0.012557T}{1-(1.52373\times10^{-3})T}\right) \tag{6}$$

The values of the effective properties employed in this investigation are obtained from following equations below. Since the density, viscosity, specific heat and conductivity of the base fluid are temperature dependent, the corresponding properties of the nanofluid are also temperature dependent. Average density and viscosity of nanofluid decrease and thermal conductivity increases along the tube. The effective physical properties of a nanofluid achieved from the physical properties of water, CuO nanoparticles and the functions of nanoparticle volume concentration (ϕ) [21]:

$$\rho_{eff} = (1-\phi)\rho_f + \phi\rho_s \tag{7}$$

$$\mu_{eff} = \left(123\phi^2 + 7.3\phi + 1\right)\mu_f \quad (8)$$

$$(C_p)_{eff} = \left[\frac{(1-\phi)(\rho C_p) + \phi(\rho C_p)_s}{(1-\phi)\rho_f + \phi\rho_s}\right] \quad (9)$$

$$\frac{k_{eff}}{k_f} = \frac{k_p + 2k_f + 2(k_p - k_f)\varphi}{k_p + 2k_f - 2(k_p - k_f)\varphi} + 5\times10^4 \beta\rho_p\varphi C_p\sqrt{\frac{k_B T}{\rho_p d_p}} f(T,\varphi) \quad (10)$$

Equations (7) and (9) are used to compute the density and specific heat for a two-phase mixture. Also, (8) for computing the dynamic viscosity of the nanofluids was obtained by performing a least-square curve fitting of experimental data available for the mixtures considered [29]. The temperature dependency of effective thermal conductivity was obtained by (10) which was presented by [30], where $f(T,\varphi) = (-6.04\varphi + 0.4705)T + (1722.3\varphi - 134.63)$ and β is a function of volume fraction. Pure water is shown by concentration of 0% which means it does not include nanoparticles.

D. Numerical Methods

The numerical method available in the commercial CFD package of ANSYS-Fluent, V14, was used in the current study. Fluent uses a finite volume approach to convert the governing partial differential equations into a system of discrete algebraic equations. In the discretization methods, a second-order upwind scheme was selected for the momentum and energy. The SIMPLE coupling algorithm was selected for single phase in order to couple pressure and velocity. The scaled residuals for the velocity components and energy are set equal to 10^{-8} and 10^{-9}, respectively.

TABLE II
BOUNDARY CONDITIONS FOR THE STRAIGHT TUBE

	Boundary conditions
Inlet	V=W=0 , T=300 k
Outlet	P=0
Wall	$u = v = w = 0,\ q_w = -k(\partial T^*/\partial r) = 0.5(W/m^2)$

E. Validation Results

A straight tube with a diameter of 10 mm and 2000 mm in length is used in the numerical study. The meshing of the straight tube consists of the grid points of 62031 and the number of elements number of 60000.

For the straight tube, the boundary conditions are shown in Table II. At The inlet, the temperature was set up to 300° K and the tube wall was exposed to 0.5 (W/m^2), uniform heat flux (qw). The numerical analyses were performed at various Reynolds numbers up to 1000 iterations until the calculated results reached to the steady state condition.

The temperature profile computed by the Ansys-Fluent and the analytical equation are shown in Fig. 4. The temperatures were calculated by using the formula nearly overlapping with the outcomes from the Fluent. The analytical solutions for the straight tube have been obtained by (11):

$$Tm(x) = Tm_i + \left(\frac{q\times p}{\dot{m}\times C_p}\right)x \quad (11)$$

The Nusselt numbers were calculated by the Fluent and the analytical solutions are presented in Fig. 5. The Nusselt numbers are gained by the software about 4.38 in the region of fully developed flow which has almost coincided with the value 4.36 from the analytical solutions with an error of 0.45%. As a result, the numerical outputs by the ANSYS-Fluent are acceptable and can be employed to analyse the nanofluid flow through an 180° curve.

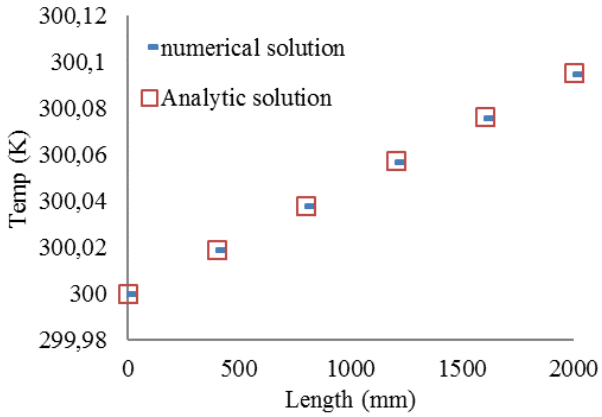

Fig. 4 Temperature profiles versus length of tube

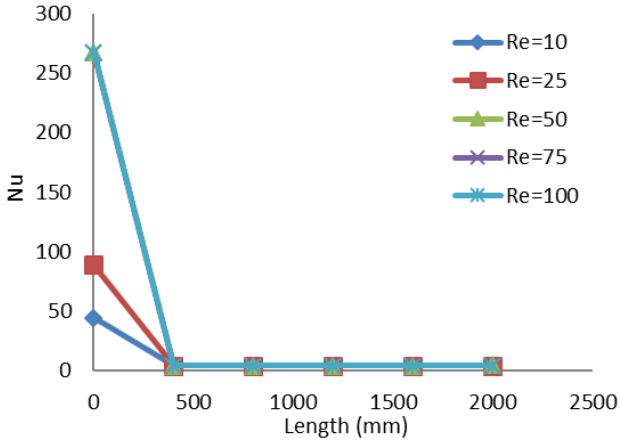

Fig. 5 Nusselt profiles at various Reynolds numbers versus length of tube

III. RESULTS AND ANALYSIS

The numerical study of developing laminar forced convection flow of a nanofluid in a circular tube with a 180 degree curve has been performed at various Reynolds numbers and concentrations. There were 25 cases of simulations where suspension concentrations of 0%, 2%, 4%, 6%, and 8% and the Reynolds numbers of 100, 250, 500, 750, and 1000 were maintained.

For a better understanding of the thermal and fluid flow in the curve, the temperature and velocity distributions for water

are shown in Figs. 6 and 7 where the Reynolds numbers are 10 and 1000, respectively. The velocity profiles are in parabolic shapes in the whole tube at the Reynolds number of 10. On the other hand, at the Reynolds number of 1000, at first the velocity close to the inner wall of the curve appears higher than that near the outer wall and then the flow changed. Fig. 8 shows the path of maximum velocity before 90 appears at the near inner wall and after 90°, the maximum velocity has moved close to the outer wall. This phenomenon improves heat transfer characteristics in the curve due to the cold flow moving to the outer region of the curve [31] as shown in Fig. 7.

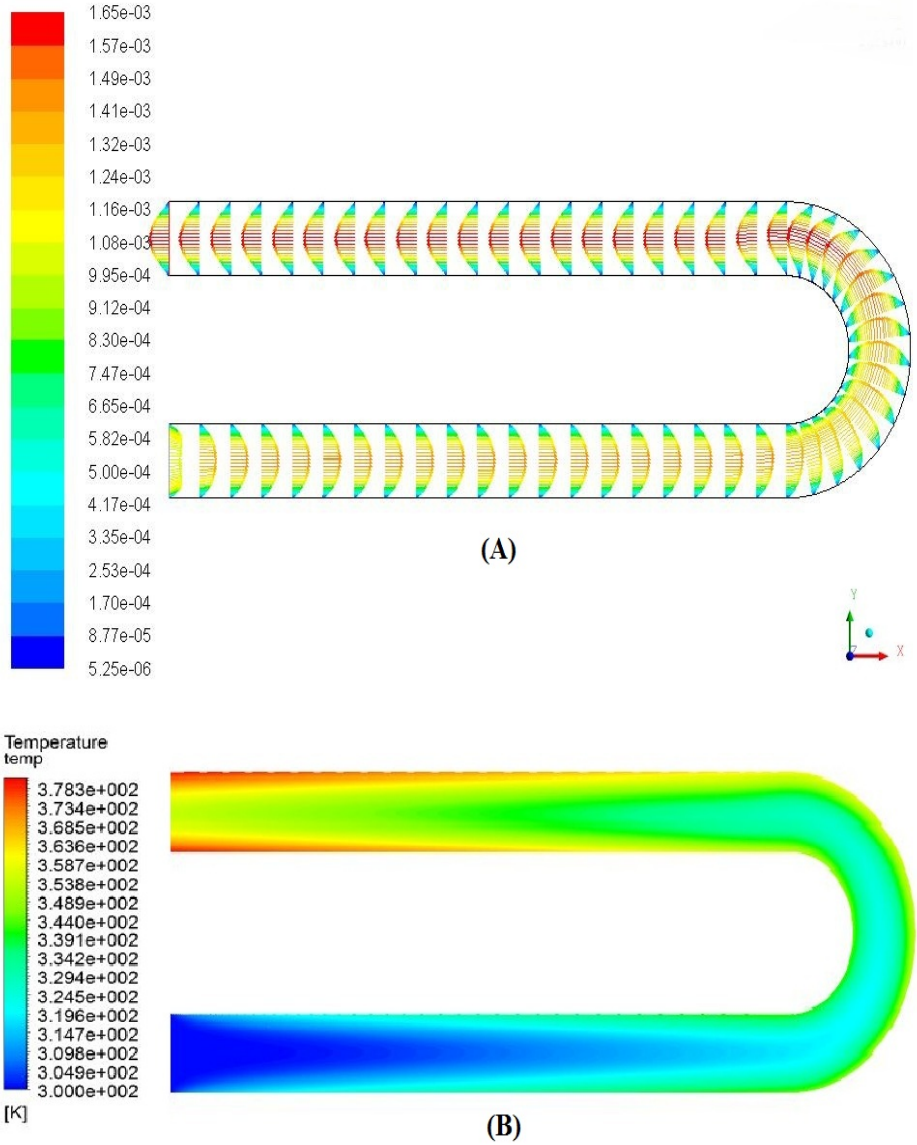

Fig. 6 Velocity Distributions (A) and temperature Distributions (B) of water at Re=10

TABLE III
INLET VELOCITIES (M/S) CHANGE WITH THE REYNOLDS NUMBERS AND CONCENTRATIONS

	0%	2%	4%	6%	8%
10	0.001004008	0.001116870	0.001343709	0.001832989	0.003334364
100	0.010040080	0.011168700	0.013437091	0.018329894	0.033343644
250	0.025100200	0.027921750	0.033592726	0.045824736	0.083359109
500	0.050200401	0.055843501	0.067185453	0.091649472	0.166718219
750	0.075300601	0.083765251	0.100778179	0.137474208	0.250077328
1000	0.100400802	0.111687001	0.134370905	0.183298944	0.333436438

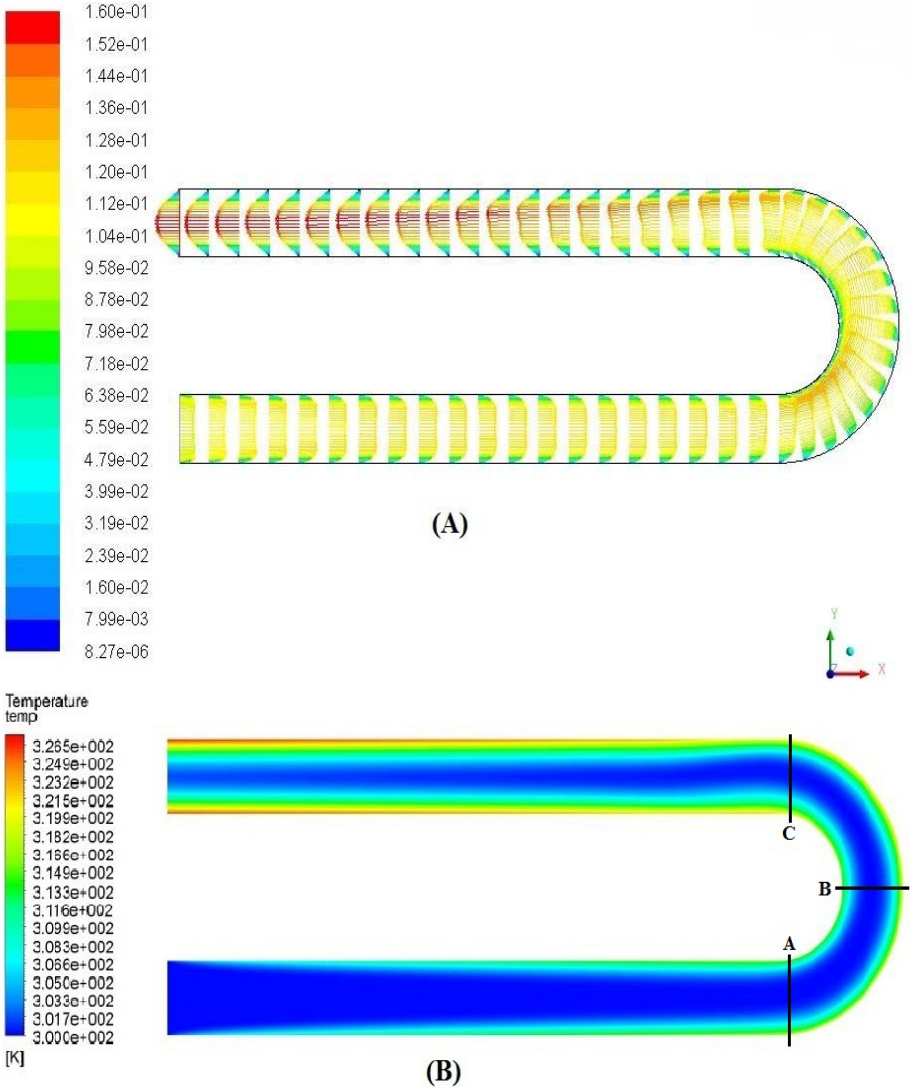

Fig. 7 Velocity Distributions (A) and temperature Distributions (B) of water at Re=1000

To look into the role of the 180 degree curve, the whole tube flow was separated into three parts of inlet tube (section A), outlet tube (section C) and the curve (section B), as shown in Fig. 8 (B). The velocity and temperature profiles at the cross sections A, B and C are presented in Figs. 9, 10 and 11, respectively.

With the increase in Reynolds number, the maximum velocity has been relocated to the outer region of the curve. As shown in Figs. 10 and 11, the temperature at the outer wall of the curve is higher than that at the centre due to the uniform heat flux, which is applied at the wall boundary. However, the temperature drops slowly with the increase in Reynolds number at outer wall of the curve because of cold flow from the inlet tube.

Centrifugal force causes secondary flow that occurred through the curve [31]. In detail, it can be seen that by increasing the inlet velocity, the cold flow transfers around the outer wall. The temperature distribution at the top of the curve is lower than at the bottom because of the gradual improvement in the secondary flow.

Fig. 12 presents the Nusselt numbers of pure water as a function of the Reynolds numbers in sections A, B and C. Although the slopes are not the same but in all sections the Nusselt numbers augmented with the inlet velocity or Reynolds number. As Fig. 7 presents that the cold flow in inlet tube moves to the outer region of the curve, as a result the Nusselt numbers of the curve (section B) at the Reynolds numbers of 100, 250, 500, 750, and 1000 are higher than the other region of the tube.

At Reynolds numbers 100, 250, 500, 750, and 1000, the average Nusselt numbers of the curve are higher than the inlet and outlet tubes due to cold flow transfers to the top of the curve as indicated in Fig. 7. In other words, due to the secondary flow, the convection in the curve enhances with the increasing Reynolds number.

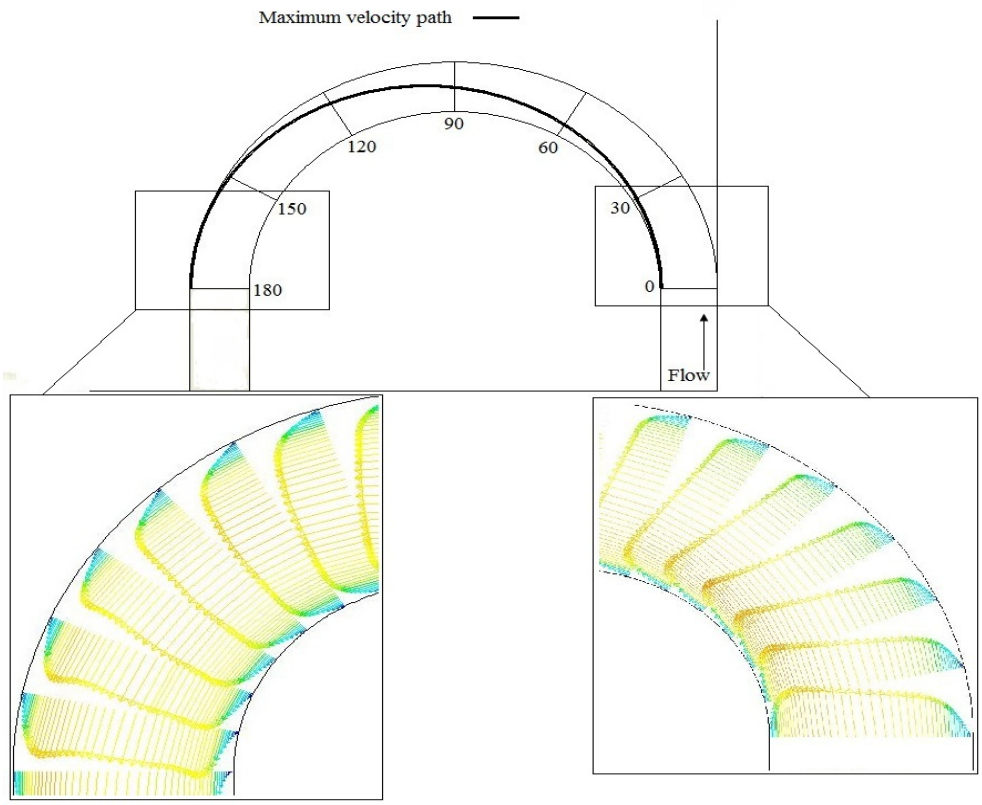

Fig. 8 Maximum velocity path at the curve section

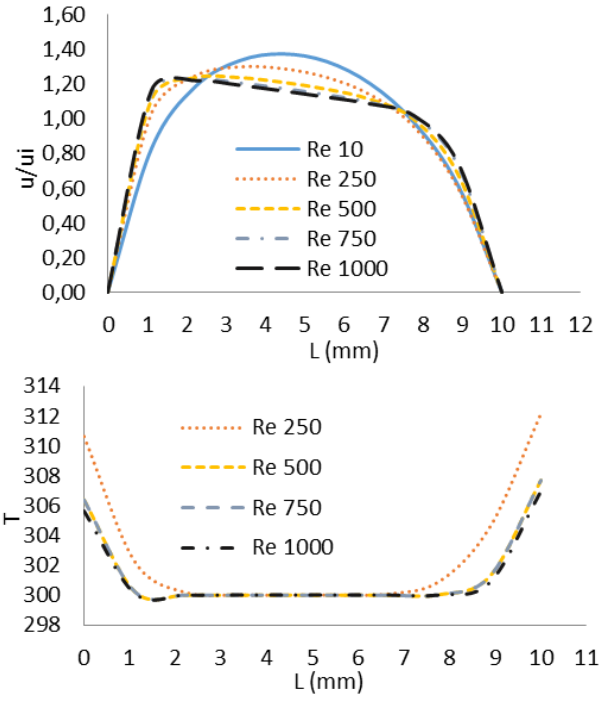

Fig. 9 Temperature and dimensionless velocity profiles at various Reynolds numbers at section (A)

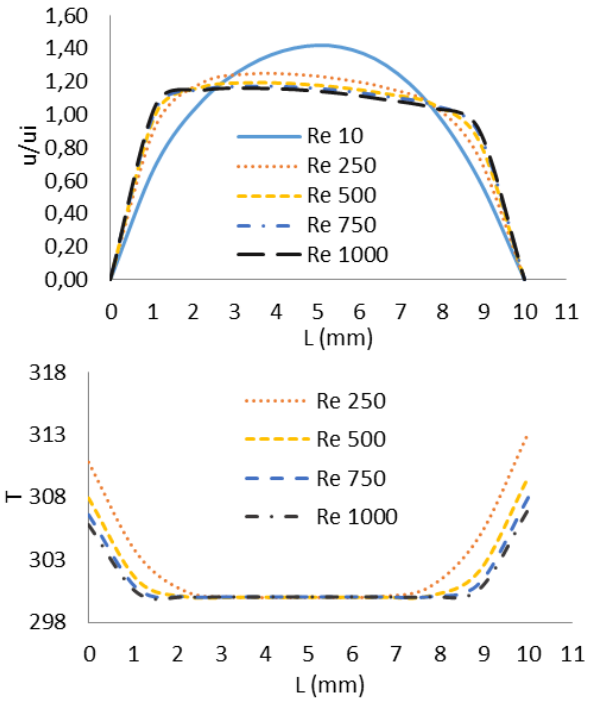

Fig. 10 Temperature and Dimensionless velocity profiles at various Reynolds numbers at section (B)

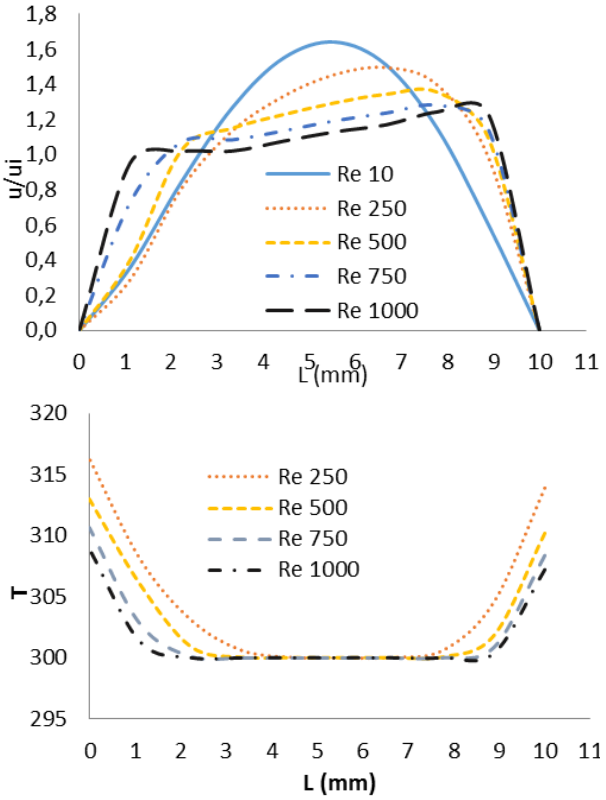

Fig. 11 Temperature and dimensionless velocity profiles at various Reynolds numbers at section (C)

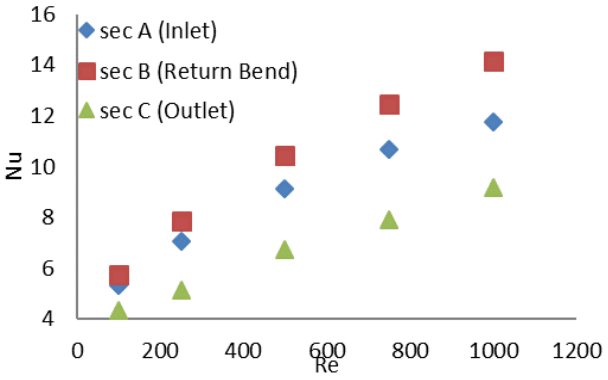

Fig. 12 Evaluations of the Nusselt numbers at section A as inlet, section C as outlet and section B as middle of the curve

Fig. 13 shows the average Nusselt numbers for various Reynolds numbers of 100, 250, 500, 750, and 1000 at the concentrations of 0%, 2%, 4%, 6%, and 8%, respectively.

The average Nusselt numbers increased with the increase in concentration and the Reynolds number. The increase in concentration leads to the enhancement of thermal conductivity and as a result heat transfer of the nanofluid. In addition, Table III indicates that at the same Reynolds number, growth of the inlet velocity is accompanied by the rise in concentration. Thus, these reasons tend to be the cause for the increase of the average Nusselt number.

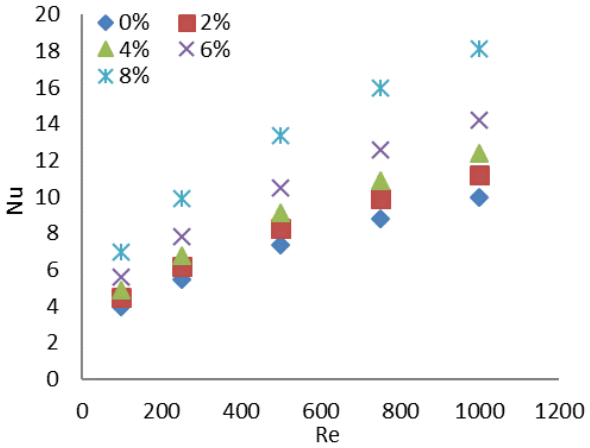

Fig. 13 Nusselt numbers at different Reynolds numbers and volume fractions in entire pipes

The pressure drop through the curve is depicted in Fig. 14. With the increase in Reynolds number pressure drop rises dramatically. Fig. 14 shows the pressure drop based on the inlet velocity. The kinematic viscosity of nanofluid leads to pressure drop at 8% concentration much higher than the pressure drop for the pure water.

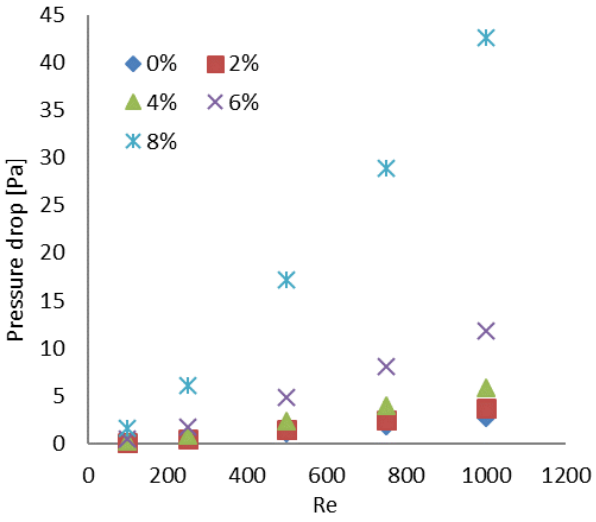

Fig. 14 Pressure drop variation at various Reynolds numbers for different concentrations

IV. Conclusion

Thermal and hydrodynamic investigations have been studied on the CuO-water based nanofluid flow through circular tube with a 180 degree curve. It could be concluded that the suspended nanoparticles significantly enhanced the heat transfer performance of the base fluid. From the results it was shown that with the increase in concentration of the thermal conductivity, the ratio of the nanofluid increases. Similarly, with the increase in volume fraction, the Nusselt number of the nanofluid increases. For the same concentration, as the Reynolds number increases, the Nusselt

number of the nanofluid increases. Thus, the heat transfer performance of the nanofluid is enhanced with the increase in the flow rate.

Practically, the heat transfer improvement in the curve is higher in comparison to the inlet and outlet tubes due to the presence of centrifugal force in the curve. Meanwhile, the volume fraction increase of the nanofluid causes the high pressure drop in the tubes. Also, pressure drop in nanofluid is higher in comparison to that in pure water.

ACKNOWLEDGMENT

The authors gratefully acknowledge Faculty of Engineering, University of Malaya, Malaysia for support to conduct this research work.

REFERENCES

[1] Prasher, R., et al., *Measurements of nanofluid viscosity and its implications for thermal applications.* Applied Physics Letters, 2006. 89(13): p. 133108.

[2] Heris, S.Z., M.N. Esfahany, and S.G. Etemad, *Experimental investigation of convective heat transfer of Al 2 O 3/water nanofluid in circular tube.* International Journal of Heat and Fluid Flow, 2007. 28(2): p. 203-210.

[3] Chon, C.H., et al., *Empirical correlation finding the role of temperature and particle size for nanofluid (Al2O3) thermal conductivity enhancement.* Applied Physics Letters, 2005. 87(15): p. 153107-153107.

[4] Nguyen, C., et al., *Viscosity data for Al 2 O 3–water nanofluid—hysteresis: is heat transfer enhancement using nanofluids reliable?* International Journal of Thermal Sciences, 2008. 47(2): p. 103-111.

[5] Yu, W., et al., *Review and comparison of nanofluid thermal conductivity and heat transfer enhancements.* Heat Transfer Engineering, 2008. 29(5): p. 432-460.

[6] Chol, S., *Enhancing thermal conductivity of fluids with nanoparticles.* ASME-Publications-Fed, 1995. 231: p. 99-106.

[7] Lotfi, R., Y. Saboohi, and A. Rashidi, *Numerical study of forced convective heat transfer of nanofluids: comparison of different approaches.* International Communications in Heat and Mass Transfer, 2010. 37(1): p. 74-78.

[8] Oztop, H.F. and E. Abu-Nada, *Numerical study of natural convection in partially heated rectangular enclosures filled with nanofluids.* International Journal of Heat and Fluid Flow, 2008. 29(5): p. 1326-1336.

[9] Jou, R.-Y. and S.-C. Tzeng, *Numerical research of nature convective heat transfer enhancement filled with nanofluids in rectangular enclosures.* International Communications in Heat and Mass Transfer, 2006. 33(6): p. 727-736.

[10] Ho, C.-J., M. Chen, and Z. Li, *Numerical simulation of natural convection of nanofluid in a square enclosure: effects due to uncertainties of viscosity and thermal conductivity.* International Journal of Heat and Mass Transfer, 2008. 51(17): p. 4506-4516.

[11] Namburu, P.K., et al., *Numerical study of turbulent flow and heat transfer characteristics of nanofluids considering variable properties.* International journal of thermal sciences, 2009. 48(2): p. 290-302.

[12] Roy, G., C.T. Nguyen, and P.-R. Lajoie, *Numerical investigation of laminar flow and heat transfer in a radial flow cooling system with the use of nanofluids.* Superlattices and Microstructures, 2004. 35(3): p. 497-511.

[13] Ding, Y., et al., *Heat transfer of aqueous suspensions of carbon nanotubes (CNT nanofluids).* International Journal of Heat and Mass Transfer, 2006. 49(1): p. 240-250.

[14] Nguyen, C.T., et al., *Heat transfer enhancement using Al_2O_3–water nanofluid for an electronic liquid cooling system.* Applied Thermal Engineering, 2007. 27(8): p. 1501-1506.

[15] Mansour, R.B., N. Galanis, and C.T. Nguyen, *Effect of uncertainties in physical properties on forced convection heat transfer with nanofluids.* Applied Thermal Engineering, 2007. 27(1): p. 240-249.

[16] Palm, S.J., G. Roy, and C.T. Nguyen, *Heat transfer enhancement with the use of nanofluids in radial flow cooling systems considering temperature-dependent properties.* Applied Thermal Engineering, 2006. 26(17): p. 2209-2218.

[17] Arzani, H.K., et al., *Experimental investigation of thermophysical properties and heat transfer rate of covalently functionalized MWCNT in an annular heat exchanger.* International Communications in Heat and Mass Transfer, 2016.

[18] Chengara, A., et al., *Spreading of nanofluids driven by the structural disjoining pressure gradient.* Journal of colloid and interface science, 2004. 280(1): p. 192-201.

[19] Wasan, D.T. and A.D. Nikolov, *Spreading of nanofluids on solids.* Nature, 2003. 423(6936): p. 156-159.

[20] You, S., J. Kim, and K. Kim, *Effect of nanoparticles on critical heat flux of water in pool boiling heat transfer.* Applied Physics Letters, 2003. 83(16): p. 3374-3376.

[21] Akbarinia, A. and A. Behzadmehr, *Numerical study of laminar mixed convection of a nanofluid in horizontal curved tubes.* Applied Thermal Engineering, 2007. 27(8): p. 1327-1337.

[22] Nnanna, A.A., et al., *Assessment of thermoelectric module with nanofluid heat exchanger.* Applied Thermal Engineering, 2009. 29(2): p. 491-500.

[23] Arzani, H.K., et al., *Experimental and numerical investigation of thermophysical properties, heat transfer and pressure drop of covalent and noncovalent functionalized graphene nanoplatelet-based water nanofluids in an annular heat exchanger.* International Communications in Heat and Mass Transfer, 2015. 68: p. 267-275.

[24] Amiri, A., et al., *Laminar convective heat transfer of hexylamine-treated MWCNTs-based turbine oil nanofluid.* Energy Conversion and Management, 2015. 105: p. 355-367.

[25] Amiri, A., et al., *Backward-facing step heat transfer of the turbulent regime for functionalized graphene nanoplatelets based water–ethylene glycol nanofluids.* International Journal of Heat and Mass Transfer, 2016. 97: p. 538-546.

[26] Xuan, Y. and Q. Li, *Investigation on convective heat transfer and flow features of nanofluids.* Journal of Heat transfer, 2003. 125(1): p. 151-155.

[27] Shih, T.M., *Numerical heat transfer*. 1984: CRC Press.

[28] Vargaftik, N.B., *Tables on the thermophysical properties of liquids and gases in normal and dissociated states.* 1975.

[29] Maïga, S.E.B., et al., *Heat transfer behaviours of nanofluids in a uniformly heated tube.* Superlattices and Microstructures, 2004. 35(3): p. 543-557.

[30] Koo, J. and C. Kleinstreuer, *A new thermal conductivity model for nanofluids.* Journal of Nanoparticle Research, 2004. 6(6): p. 577-588.

[31] Ghobadian, R. and K. Mohammadi, *Simulation of subcritical flow pattern in 180 uniform and convergent open-channel bends using SSIIM 3-D model.* 水科学与水工程, 2011. 4(3).